Influence of dynamical parameters on pre-scission particles and fission probability in heavy-ion collisions

M. R. Pahlavani* and D. Naderi†

Department of Physics, Faculty of Basic Science, Mazandaran University, P.O. Box 47416-1467, Babolsar, Iran

(Received 2 August 2010; published 3 February 2011)

A stochastic approach to fission dynamics based on one- and three-dimensional Langevin equations was applied to calculate the fission probability and the pre-scission particle multiplicity. Evaporation of pre-scission light particles along Langevin fission trajectories from the ground state of the compound nucleus to its scission and fission probability have been calculated using a Monte Carlo simulation technique. To examine this approach we used $^{19}F + ^{181}Ta$ and $^{16}O + ^{197}Au$ systems. Our results show that the fission probability and pre-scission particle multiplicity in three dimensions is different from the one-dimensional Langevin approach. The theoretical results of pre-scission neutron, proton, and α-particle multiplicities and the fission probability for given systems based on this model are compared with available experimental data. The obtained results using three-dimensional calculations are in better agreement with experimental data.

DOI: 10.1103/PhysRevC.83.024602 PACS number(s): 25.70.Jj, 24.75.+i, 05.10.Gg

I. INTRODUCTION

Studies on the nature and magnitude of nuclear dissipation have attracted considerable interest in recent years [1–6]. It is well established that the dissipation causes the delay of the fission process [7–9] with respect to the statistical picture of compound nucleus decay and has an impact on many experimental observables, such as pre-scission particle multiplicities, fission probability, and the mass-energy distribution of fission fragments. The emission of light particles, especially neutrons that act as a clock to measure the fission time scale, has proved to be very useful in investigating the mechanism of nuclear fission [10,11]; e.g., an important fact is that the nuclear temperature decreases as the neutrons are emitted, removing kinetic energy from the fissioning nucleus. The observed neutron multiplicity emitted prior to scission is larger than the result calculated by the statistical model of Bohr and Wheeler [12].

Many recent studies have demonstrated the successful application of the multidimensional Langevin equations to the fission of an excited compound nuclei formed in reactions induced by heavy ions [10,13–15]. From the physical point of view, the Langevin equations are equivalent to the Fokker-Planck equation, which is widely used for modeling the fission of excited nuclei in the framework of the diffusion model. In contrast to models based on the Fokker-Planck equation, the multidimensional Langevin equations are more suitable for computer modeling and do not require extra assumptions and approximations during the integration procedure.

Ye and co-authors have proposed many one-dimensional dynamical fission calculations to investigate the sensitivity of the pre-scission particle, γ-ray [16–19], and evaporation-residue cross sections [20,21] by considering the isospin of the compound nucleus and viscosity as effective parameters. Nearly all the problems in collective nuclear dynamics are essentially multidimensional. However, one-dimensional calculations can be used for the theoretical investigation of pre-scission particle emission and time characteristics of the fission process. Ying Jia and Jing Dong Bao [22] have calculated the pre-scission neutron multiplicity and anisotropy using Langevin equations with one and two dimensions. They show that their results for a two-dimensional model are in better agreement with the experimental data. However, studies based on the influence of the dimensionality of the dynamical model on the pre-scission particles and fission probability have not yet been performed.

In this study we performed one- and three-dimensional dynamical calculations to investigate the influence of dimensionality of the dynamical model on the pre-scission neutron, proton, α-particle, and fission probability. The paper is organized as follows. In Sec. II, we describe the model, basic equation, and parameters. Results obtained based on this model compared with experimental data are presented in Sec. III. Finally, concluding remarks are given in Sec. IV.

II. MODEL CONSIDERATIONS

In our model we used the (c, h, α) parametrization, in which c denotes the elongation parameter, h is the variation in the thickness of the neck for a given elongation of the nucleus, and α is the asymmetry parameter. The equation of the nuclear surface in cylindrical coordinates is given by [23]

$$\rho_s^2(z) = (c^2 - z^2)(A/c^2 + Bz^2/c^2 + \alpha z/c), \qquad (1)$$

where ρ_s and z are radial and parallel coordinates relative to the symmetry or fission axis, respectively. A and B are defined in Ref. [23]. The neck thickness and asymmetry parameter of fissioning nucleus can be defined by [23]

$$h = -1.047c^3 + 4.297c^2 - 6.309c + 4.073 \qquad (2)$$

and

$$\alpha = 0.11937\alpha_{as}^2 + 0.24720\alpha_{as}, \qquad (3)$$

*m.pahlavani@umz.ac.ir
†d.naderi@umz.ac.ir

where

$$\alpha_{\rm as} = \frac{A_1 - A_2}{A}. \tag{4}$$

In this relation A_1 and A_2 are the mass numbers of the fission fragments.

The coupled Langevin used in this model reads [24]

$$\begin{aligned} \frac{dq_i}{dt} &= \mu_{ij} p_j, \\ \frac{dp_i}{dt} &= -\frac{p_j p_k}{2}\frac{\partial \mu_{jk}}{\partial q_i} - \frac{\partial F}{\partial q_i} - \gamma_{ij}\mu_{jk} p_j + R(t), \end{aligned} \tag{5}$$

where q_i is the vectors of the collective coordinate, and p_i are their conjugate momenta. $F(q) = V(q) - a(q)T^2$ is the Helmholtz free energy. $V(q)$ is the potential energy, $m_{ij}(q)(\|\mu_{ij}\| = \|m_{ij}\|^{-1})$ is the tensor of inertia, $\gamma_{ij}(q)$ is the friction tensor, and $R(t)$ represents the random part of the interaction between the fission degree of freedom and the thermal bath [24]. The temperature T of the heat bath is determined by the Fermi-gas model formula

$$T = \sqrt{E_{\rm int}/a(q)}, \tag{6}$$

where $E_{\rm int}$ is the internal excitation energy of nucleus, and $a(q)$ is the level density parameter [25]. During a random walk along the Langevin trajectory, conservation of energy is satisfied by

$$E^* = E_{\rm int} + E_{\rm coll} + V(q) + E_{\rm evap}(t), \tag{7}$$

where E^* is the total excitation energy of the compound nucleus, $E_{\rm coll}$ is the kinetic energy of the collective degrees of freedom, and $E_{\rm evap}$ is the energy carried out by evaporated particles.

The friction tensor in the one-body dissipation scheme for small elongation before neck formation ($c < c_{\rm win}$) can be written as [26]

$$\begin{aligned} \gamma_{ij}^{\rm wall}(c < c_{\rm win}) = \frac{\pi}{2}\rho_m \overline{\upsilon} \int_{z_{\rm min}}^{z_{\rm max}} \left(\frac{\partial \rho_s^2}{\partial q_i}\right)\left(\frac{\partial \rho_s^2}{\partial q_j}\right) \\ \times \left[\rho_s^2 + \left(\frac{1}{2}\frac{\partial \rho_s^2}{\partial z}\right)^2\right]^{-1/2} dz, \end{aligned} \tag{8}$$

and for further elongation in which a neck is formed ($c > c_{\rm win}$), the corresponding friction tensor can be written as [26]

$$\begin{aligned} &\gamma_{ij}^{\rm wall}(c \geqslant c_{\rm win}) \\ &= \frac{\pi}{2}\rho_m \overline{\upsilon} \left\{ \int_{z_{\rm min}}^{z_{\rm neck}} \left(\frac{\partial \rho_s^2}{\partial q_i} + \frac{\partial \rho_s^2}{\partial z}\frac{\partial D_1}{\partial q_i}\right)\left(\frac{\partial \rho_s^2}{\partial q_j} + \frac{\partial \rho_s^2}{\partial z}\frac{\partial D_1}{\partial q_j}\right) \right. \\ &\times \left[\rho_s^2 + \left(\frac{1}{2}\frac{\partial \rho_s^2}{\partial z}\right)^2\right]^{-1/2} dz + \int_{z_{\rm neck}}^{z_{\rm max}} \left(\frac{\partial \rho_s^2}{\partial q_i} + \frac{\partial \rho_s^2}{\partial z}\frac{\partial D_2}{\partial q_i}\right) \\ &\left. \times \left(\frac{\partial \rho_s^2}{\partial q_j} + \frac{\partial \rho_s^2}{\partial z}\frac{\partial D_2}{\partial q_j}\right)\left[\rho_s^2 + \left(\frac{1}{2}\frac{\partial \rho_s^2}{\partial z}\right)^2\right]^{-1/2} dz \right\}, \end{aligned} \tag{9}$$

$$\gamma_{ij}^{\rm win}(c \geqslant c_{\rm win}) = \frac{\pi}{2}\rho_m \overline{\upsilon}\left(\frac{\partial R}{\partial q_i}\frac{\partial R}{\partial q_j}\right)\Delta\sigma. \tag{10}$$

Here ρ_m is the mass density of the nucleus, $\overline{\upsilon}$ is the average nucleon speed inside the nucleus, and D_1, D_2 are the position of the centers of two parts of the fissioning system relative to the center of mass of the whole system. $z_{\rm min}$ and $z_{\rm max}$ are two extreme ends of the nuclear shape along the z axis and $z_{\rm neck}$ is the position of neck plane that divides the nucleus into two parts. $\Delta\sigma$ is the area of the window between two parts of the system and R is the distance between centers of mass of nascent fragments.

The wall friction is modified by a chaoticity factor (μ), which gives the average fraction of trajectories which are chaotic when sampling is done uniformly over the surface. In other words, the chaoticity is used to express the degree of irregularity in the dynamics of the system. Each such trajectory is identified as a regular or as a chaotic one by considering the magnitude of its Lyapunov exponent over a long time interval [27]. This modified or scaled version of the wall friction is known as the chaos-weighted wall friction [28]:

$$\gamma_{ij}(c < c_{\rm win}) = \mu(c)\gamma_{ij}^{\rm wall}(c < c_{\rm win}), \tag{11}$$

$$\gamma_{ij}(c \geqslant c_{\rm win}) = \mu(c)\gamma_{ij}^{\rm wall}(c \geqslant c_{\rm win}) + \gamma_{ij}^{\rm win}(c \geqslant c_{\rm win}), \tag{12}$$

where the value of μ changes from 0 to 1 as the nucleus evolves from spherical to a deformed shape.

The angular momentum l for each Langevin trajectory is simulated by the Monte Carlo method from the triangular spin distribution function with the maximum critical angular momentum l_c for fusion. This function is defined by [11]

$$\frac{d\sigma(l)}{dl} = \frac{2\pi}{k^2}\frac{2l+1}{1+\exp[(l-l_c)/\delta l]}. \tag{13}$$

The particle emission width for a particle of kind ν is given by [11]

$$\begin{aligned} \Gamma_\nu = (2s_\nu + 1)\frac{m_\nu}{\pi^2\hbar^2\rho_c(E^*)} \\ \times \int_0^{E^*-B_\nu} \rho_R(E^* - \varepsilon_\upsilon)\varepsilon_\upsilon\sigma_{\rm inv}(\varepsilon_\upsilon)d\varepsilon_\nu, \end{aligned} \tag{14}$$

where s_ν is the spin of the emitted particle ν and m_ν is its reduced mass with respect to the residual nucleus. The level densities of the compound and residual nuclei are denoted by $\rho_c(E^*)$ and $\rho_R(E^* - \varepsilon_\nu)$, respectively. The intrinsic energy is E^*, and B_ν are the liquid drop binding energies according to Refs. [29,30]. The inverse cross sections are given by [31]

$$\sigma_{\rm inv}(\varepsilon_\nu) = \begin{cases} \pi R_\nu^2(1 - V_\nu/\varepsilon_\nu), & \varepsilon_\nu > V_\nu, \\ 0, & \varepsilon_\nu < V_\nu, \end{cases} \tag{15}$$

with

$$R_\nu = 1.21\left[(A - A_\nu)^{1/3} + A_\nu^{1/3}\right] + \left(3.4/\varepsilon_\nu^{1/2}\right)\delta_{\nu,n}, \quad (16)$$

where A_ν is the mass number of the emitted particle $\nu = n, p, \alpha$. The considered barriers for the charged particles are

$$V_\nu = [(Z - Z_\nu)Z_\nu K_\nu]/(R_\nu + 1.6), \quad (17)$$

with $K_\nu = 1.32$ for α particles and 1.15 for protons.

For γ-ray multiplicity the ground state to saddle point evaluation of the compound nucleus contributes much more than the saddle to scission point. In other words, we considered only γ rays which are emitted at the beginning of the process. For the emission of giant dipole γ quanta we used the formula given by Lynn [32]:

$$\Gamma_\gamma = \frac{3}{\rho_c(E^*)}\int_0^{E^*} d\varepsilon \rho_c(E^* - \varepsilon) f(\varepsilon), \quad (18)$$

where ε is the energy of the emitted γ ray and $f(\varepsilon)$ is defined by [32]

$$f(\varepsilon) = \frac{4}{3\pi}\frac{1+k}{mc^2}\frac{e^2}{\hbar c}\frac{NZ}{A}\frac{\Gamma_G \varepsilon^4}{(\Gamma_G\varepsilon)^2 + \left(\varepsilon^2 - E_G^2\right)^2}, \quad (19)$$

with $E_G = 80A^{-1/3}$ MeV and $\Gamma_G = 5$ MeV being the position and width of the giant dipole resonance and $k = 0.75$ [33]. Also A, Z, and N refer to mass, charge, and neutron number of compound nucleus, respectively.

A Monte Carlo algorithm is used to calculate the competition among particle emission, γ-ray emission, and fission. In the first step a random number r on the interval (0, 1) is chosen based on a Monte Carlo technique. This random number is a numerical characteristic assigned to an element of the sample space. Then we define the probability of emission of a particle as $x = \tau/(\hbar/\Gamma_R)$, where $\Gamma_R = \Gamma_n + \Gamma_p + \Gamma_\alpha + \Gamma_\gamma$ and τ is the time step of the calculation. Values of $r < x$ are interpreted as particle emissions. In each time interval only the emission of one particle is considered.

In the case when a particle is emitted, the type of emitted particle is then decided by a Monte Carlo selection with the weights Γ_ν/Γ_R ($\nu = n, p, \alpha, \gamma$). After each emission the intrinsic excitation energy of the residual mass and spin of the compound nucleus is recalculated based on the energy removed by one particle emission. The spin of the compound nucleus is reduced by assuming that each neutron, proton, or a γ ray carries away $1\hbar$ while the α particle carries away $2\hbar$ of angular momentum. This cycle of calculations is repeated for typically 50 000 Langevin trajectories and until it reaches a scission point criteria ($c = c_{\rm sci}$) [23]

$$c_{\rm sci} = -2.0\alpha^2 + 0.032\alpha + 2.0917. \quad (20)$$

The pre-scission particle multiplicities have been calculated for each α and finally these multiplicities are averaged to obtained the pre-scission particle multiplicities. In one-dimensional Langevin calculations, we used the elongation parameter c as a collective coordinate, while the parameters h and α have been set to zero. The three-dimensional Langevin calculations were performed using the collective coordinates c, h, and α.

We obtained average values of the different quantities using the following relation:

$$\langle\xi\rangle = \frac{\sum_l \sum_\alpha \langle\xi\rangle_{l,\alpha}(2l+1)P_l}{\sum_l \sum_\alpha (2l+1)P_l}. \quad (21)$$

The quantity ξ can be any of the parameters $M_n^{\rm Pre}$, $M_p^{\rm Pre}$, and $M_\alpha^{\rm Pre}$. Also, P_l is the probability of a particle crossing the fission barrier, which depends upon angular momentum, and is calculated using

$$P_l = \frac{N_l}{N}, \quad (22)$$

where N and N_l are the total number of trajectories and the number of trajectories which undergo fission, respectively.

Summation over the asymmetry parameter is defined in an interval $[0, \alpha]$ and summation over l is defined in an interval $[0, l_f]$, where α_f and l_f refer to maximum asymmetry and critical angular momentum for fusion, respectively.

III. RESULTS

The systems typically chosen for the present work are ^{19}F + ^{181}Ta and ^{16}O + ^{197}Au because of the ample experimental data available for them in the literature. The calculated pre-scission neutron, proton, and α-particle multiplicities are plotted along with the respective experimental data versus energy of the compound system for comparison in Figs. 1–6. The variations of pre-scission neutron multiplicity as a function of energy for ^{19}F + ^{181}Ta and ^{16}O + ^{197}Au reactions are shown in Figs. 1 and 2, respectively. At lower energies the difference between theoretical results based on Langevin dynamics and experimental data is lower but at higher energies the results based on three-dimensional calculations are lower than those from one-dimensional ones and consequently are in better agreement with experimental data.

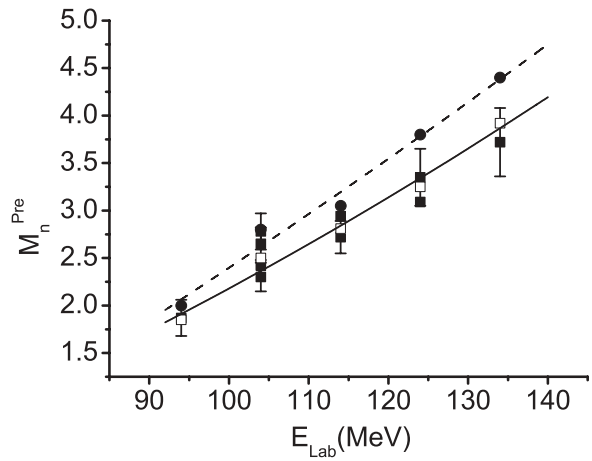

FIG. 1. Pre-scission multiplicity as function of energy for ^{19}F + ^{181}Ta reaction. Filled squares show experimental data [34]. Filled circles and open squares represent theoretical calculations based on one- and three-dimensional Langevin approaches, respectively. The dashed and solid lines are approximation of, respectively, one- and three-dimensional Langevins by a polynomial of second order.

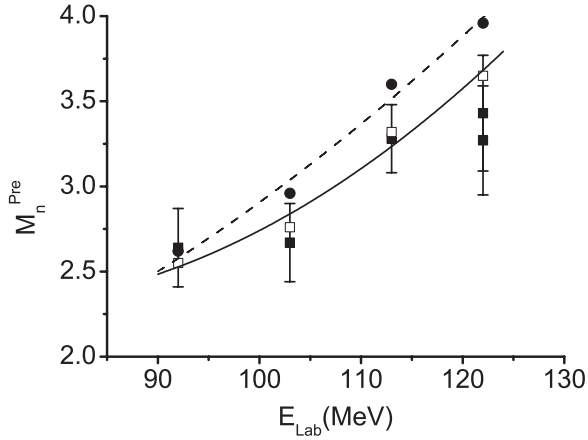

FIG. 2. Pre-scission multiplicity as function of energy for $^{16}O + ^{197}Au$ reaction. Filled squares show experimental data [34]. Filled circles and open squares represent theoretical calculations based on one- and three-dimensional Langevin approaches, respectively. The dashed and solid curves are approximation of, respectively, one- and three-dimensional Langevins by a polynomial of second order.

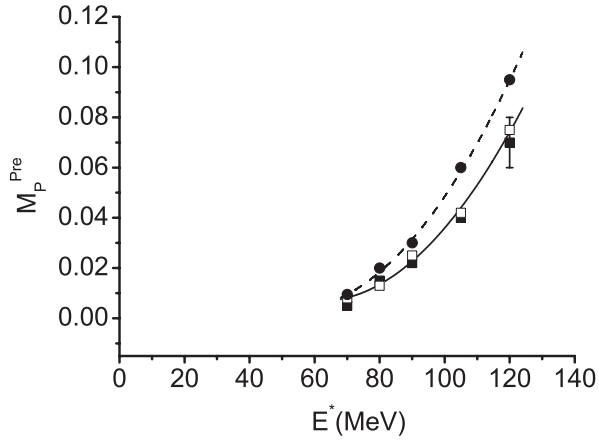

FIG. 4. Pre-scission proton multiplicity vs excitation energy for the $^{19}F + ^{181}Ta$ reaction. The experimental data (filled squares) are taken from Ref. [35]. Filled circles and open squares show results of one- and three-dimensional Langevin approaches, respectively. The dashed and solid curves are approximation of, respectively, one- and three-dimensional Langevins by a polynomial of second order.

In Figs. 3 and 4 the variation of pre-scission proton multiplicity is presented as a function of excitation energy for $^{16}O + ^{197}Au$ and $^{19}F + ^{181}Ta$ reactions, respectively. The obtained results for proton multiplicity based on one- and three-dimensional approaches are close to each other (at lower and medium energy); however, three-dimensional results are in better agreement with experimental data. The variation of pre-scission α-particle multiplicity is plotted as a function of excitation energy for $^{16}O + ^{197}Au$ and $^{19}F + ^{181}Ta$ reactions in Figs. 5 and 6, respectively. With an increase in excitation energy, theoretical calculations without including neck thickness and asymmetry (dashed curves in Figs. 5 and 6) systematically overestimate the experimental pre-scission α-particle multiplicities. By using neck thickness and asymmetry parameters in calculations (solid curves in Figs. 5 and 6) the agreement between theoretical and experimental results can be reasonably well explained.

We studied the fission probability of the two systems as a function of excitation energy. The results are shown in Figs. 7 and 8. The results obtained from the one-dimensional calculations are lower than those of the three-dimensional calculations. The agrement between theoretical results based on a three-dimensional calcualtion and experimental data is satisfactory. The difference between the fission probability in the two models is caused by the fission rate being larger in three-dimensional calculations than in one-dimensional calculations. We calculated the probability of the system remaining as a compound nucleus, $P_{C.N.}$, i.e., the number of samples with $c < c_{scis}$ divided by the total number of samples, and then calculated the fission rate as $r(t) = -(1/P_{CN})\, dP_{CN}/dt$. The

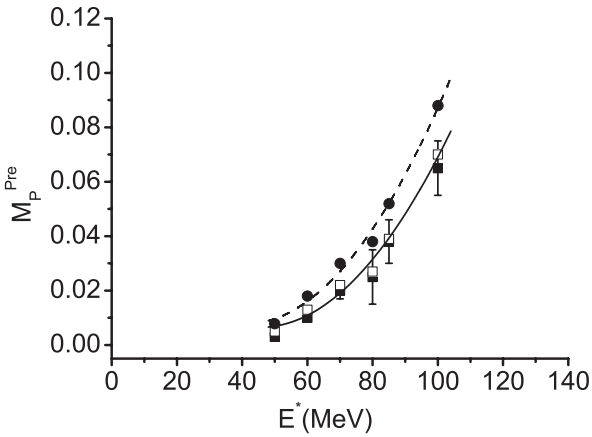

FIG. 3. Pre-scission proton multiplicity as a function of excitation energy for the $^{16}O + ^{197}Au$ reaction. Filled squares show experimental data [35]. Filled circles and open squares show results of one- and three-dimensional Langevin approaches, respectively. The dashed and solid curves are approximations of, respectively, one- and three-dimensional Langevins by a polynomial of second order.

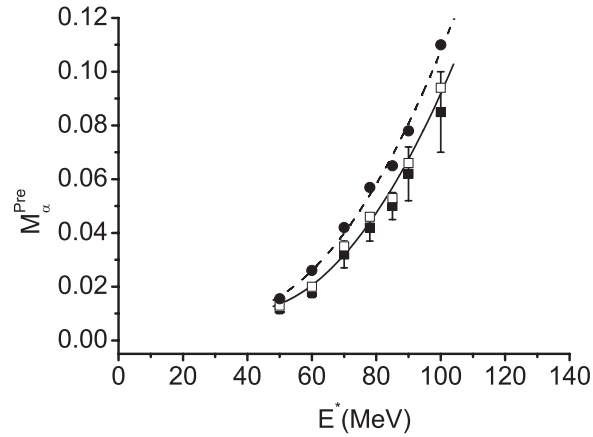

FIG. 5. Pre-scission α-particle multiplicity as a function of excitation energy for the $^{16}O + ^{197}Au$ reaction. Filled squares show experimental data [35]. Filled circles and open squares show results of one- and three-dimensional Langevin approaches, respectively. The dashed and solid curves are approximations of, respectively, one- and three-dimensional Langevins by a polynomial of second order.

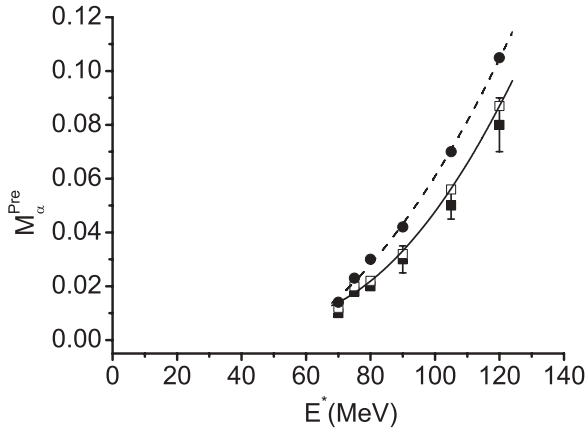

FIG. 6. Pre-scission α-particle multiplicity vs excitation energy for the $^{19}F + ^{181}Ta$ reaction. The experimental data (filled squares) are taken from Ref. [35]. Filled circles and open squares show results of one- and three-dimensional Langevin approaches, respectively. The dashed and solid curves are approximations of, respectively, one- and three-dimensional Langevins by a polynomial of second order.

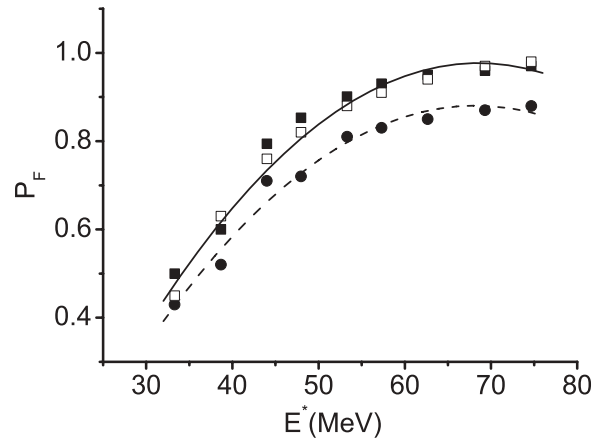

FIG. 8. Fission probability vs excitation energy for the $^{16}O + ^{197}Au$ reaction. The experimental data (filled squares) are taken from Ref. [38]. Filled circles and open squares show results of one- and three-dimensional Langevin approaches, respectively. The dashed and solid curves are approximations of, respectively, one- and three-dimensional Langevins by a polynomial of second order.

fission rate is analyzed in terms of the stationary value and the transient time. The transient time is the time needed for the $r(t)$ to reach 90% of the stationary value and is obtained as $\tau_f = \beta/2\omega^2 \ln(10b_f/T)$ [9], where β represents the dissipation strength, ω defines the potential inside the barrier, b_f is the fission barrier hight, and T is the nuclear temperature. Our study shows that the transient time is larger for three-dimensional calculations. This result reflects the fact that three-dimensional trajectories explore a large phase space compared to those in one dimension before they reach the scission configuration, resulting in an additional delay for the former.

The change in the stationary value of the fission rate when going from a one-dimensional to a three-dimensional description can be caused by both static and dynamic characteristics of the fission process. In Ref. [37] the influence of the geometry of the fission valley on the calculated value of the stationary fission rate has been discussed. It was shown that if the fission valley gets wider as one approaches the saddle-point configuration, the three-dimensional stationary value of the fission rate will increase by up to 50% as compared to the one-dimensional value. The opposite is to be expected if the fission valley gets narrower when approaching the saddle-point configuration. Apart from these static arguments, in the three-dimensional Langevin model the stationary value of the fission width will also be influenced by the dependence of the mass and friction tensors on the chosen collective variables. The combination of all these effects leads to the differences between the one- and three-dimensional results, as is clear in Figs. 7 and 8.

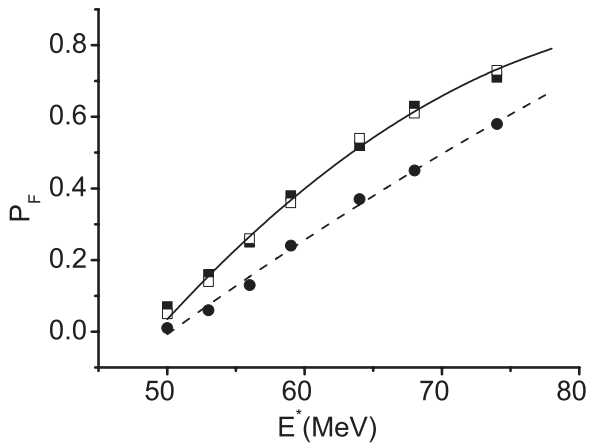

FIG. 7. Fission probability vs excitation energy for the $^{19}F + ^{181}Ta$ reaction. Filled squares show experimental data [36]. Filled circles and open squares show results of one- and three-dimensional Langevin approaches, respectively. The dashed and solid curves are approximations of, respectively, one- and three-dimensional Langevins by a polynomial of second order.

IV. SUMMARY AND CONCLUSION

In conclusion, we have developed two dynamical model (one- and three-dimensional Langevin models) for fission where fission trajectories are generated through solving Langevin equations with dissipative forces and by considering asymmetric mass division of fragments and nonconstant viscosity to simulate the pre-scission particle emission through a Monte Carlo simulation technique. The results based on a three-dimensional Langevin approach compared with a one-dimensional Langevin approach are in better agreement with experimental data. For pre-scission particles at lower energies the results of the two models are almost identical but at medium and higher energies the results of the one-dimensional calculation give higher values than in the three-dimensional case. Also, one can conclude that considering the neck thickness and asymmetry degrees of freedom decreases the pre-scission particle multiplicities. For the pre-scission configuration particle multiplicity is lower for three-dimensional calculations compared with one dimensional. It is evident that each emission of a light particle carries away

excitation energy and angular momentum, thereby increasing the height of the fission barrier of the residual nucleus, which, in turn, renders the fission event less and less probable. Also, the difference between the fission probability in the two models is caused by the fission rate in the three-dimensional model being larger than in the one-dimensional model. Also, our results agree with theoretical investigations by other authors on other systems, in particular the work of Natdtochy *et al.* [24].

[1] J. Sadhukhan and S. Pal, Phys. Rev. C **78**, 011603(R) (2008).
[2] J. U. Andersen *et al.*, Phys. Rev. C **78**, 064609 (2008).
[3] C. Schmitt, P. N. Nadtochy, A. Heinz, B. Jurado, A. Kelic, and K. H. Schmidt, Phys. Rev. Lett. **99**, 042701 (2007).
[4] B. Jurado, C. Schmitt, K.-H. Schmidt, J. Benlliure, T. Enqvist, A. R. Junghans, A. Kelić, and F. Rejmund, Phys. Rev. Lett. **93**, 072501 (2004).
[5] V. Tishchenko, C.-M. Herbach, D. Hilscher, U. Jahnke, J. Galin, F. Goldenbaum, A. Letourneau, and W.-U. Schröder, Phys. Rev. Lett. **95**, 162701 (2005).
[6] S. M. Mirfathi and M. R. Pahlavani, Phys. Rev. C **78**, 064612 (2008).
[7] D. J. Hinde *et al.*, Nucl. Phys. A **502**, 497c (1989).
[8] P. Grangé, L. Jun-Qing, and H. A. Weidenmüller, Phys. Rev. C **27**, 2063 (1983).
[9] K. H. Bhatt, P. Grangé, and B. Hiller, Phys. Rev. C **33**, 954 (1986).
[10] Y. Abe, S. Ayik, P. G. Reinhard, and E. Suraud, Phys. Rep. **275**, 49 (1996).
[11] P. Fröbrich and I. I. Gontchar, Phys. Rep. **292**, 131 (1998).
[12] M. Thoennessen and G. F. Bertsch, Phys. Rev. Lett. **71**, 4303 (1993).
[13] A. V. Karpov, R. M. Hiryanov, A. V. Sagdeev, and G. D. Adeev, J. Phys. G: Nucl. Part. Phys. **34**, 255 (2007).
[14] A. V. Karpov, P. N. Nadtochy, D. V. Vanin, and G. D. Adeev, Phys. Rev. C **63**, 054610 (2001).
[15] P. N. Nadtochy, G. D. Adeev, and A. V. Karpov, Phys. Rev. C **65**, 064615 (2002).
[16] W. Ye, F. Wu, and H. W. Yang, Phys. Lett. B **647**, 118 (2007).
[17] W. Ye, Phys. Rev. C **80**, 011601(R) (2009).
[18] N. Chen and Y. Wei, Commun. Theor. Phys. (Beijing, China) **52**, 329 (2009).
[19] W. Ye, Int. J. Mod. Phys. E **12**, 817 (2003).
[20] W. Ye, Phys. Rev. C **76**, 021604(R) (2007).
[21] W. Ye, H. W. Yang, and F. Wu, Phys. Rev. C **77**, 011302(R) (2008).
[22] Y. Jia and J.-D. Bao, Phys. Rev. C **75**, 034601 (2007).
[23] A. K. Dhara, K. Krishan, C. Bhattacharya, and S. Bhattacharya, Phys. Rev. C **57**, 2453 (1998).
[24] P. N. Nadtochy *et al.*, Phys. Lett. B **685**, 258 (2010).
[25] A. V. Ignatyuk, M. G. Itkis, V. N. Okolovich, G. N. Smirenkin, and A. S. Tishin, Yad. Fiz. **21**, 1185 (1975) [Sov. J. Nucl. Phys. **21**, 612 (1975)].
[26] D. V. Vanin, G. I. Kosenko, and G. D. Adeev, Phys. Rev. C **59**, 2114 (1999).
[27] J. Blocki, F. Brut, T. Srokowski, and W. J. Swiatecki, Nucl. Phys. A **545**, 511c (1992).
[28] S. Pal and T. Mukhopadhyay, Phys. Rev. C **57**, 210 (1998).
[29] W. D. Myers and W. J. Swiatecki, Nucl. Phys. **81**, 60 (1966).
[30] W. D. Myers and W. J. Swiatecki, Ark. Fys. **36**, 343 (1967).
[31] M. Blann, Phys. Rev. C **21**, 1770 (1980).
[32] J. E. Lynn, ed., *The Theory of Neutron Resonance Reactions* (Clarendon, Oxford, 1968), p. 325.
[33] V. G. Nedoresov, Yu. N. Ranyuk, *Fotodelenie Yader za Gigantskim Rezonansom* (Kiev, Naukova Dumka, 1989) (in Russian).
[34] J. O. Newton, D. J. Hinde, R. J. Charity, J. R. Leigh, J. J. M. Bokhorst, A. Chatterjee, G. S. Foote, and S. Ogaza, Nucl. Phys. A **483**, 126 (1988).
[35] H. Ikezoe, N. Shikazono, Y. Nagame, T. Ohtsuki, Y. Sugiyama, Y. Tomita, K. Ideno, I. Kanno, H. J. Kim, B. J. Qi, and A. Iwamoto, Nucl. Phys. A **538**, 299c (1992).
[36] J. S. Forster, I. V. Mitchell, J. U. Andersen, A. S. Jensen, E. Laegsgaard, W. M. Gibson, and K. Reichelt, Nucl. Phys. A **464**, 497 (1987).
[37] H. A. Weidenmüller and Z. Jing-Shang, J. Stat. Phys. **34**, 191 (1984).
[38] D. J. Hinde, R. J. Charity, G. S. Foote, J. R. Leigh, J. O. Newton, S. Ogaza, and A. Chattejee, Nucl. Phys. A **452**, 550 (1986).